J Ther Eng, Vol. 8, No. 2, pp. 286–298, March 2022

Journal of Thermal Engineering
Web page info: https://jten.yildiz.edu.tr
DOI: 10.18186/thermal.1086264

Journal of Thermal Engineering

Research Article

Three dimensional MHD nano luid stagnation point low with higher order chemical reaction

S. JAGADHA[1], D. GOPAL[2], P. Vijay KUMAR[3], N. KISHAN[2], P. DURGAPRASAD[3]*

[1]*Department of Mathematics, Institute of Aeronautical Engineering, Dundigal, Hyderabad, T.S, India*
[2]*Department of Mathematics, UCS, Osmania University, Hyderabad, Telangana, India*
[3]*Mathematics Division, School of Advanced sciences, VIT Chennai Campus, T.N, India*

ARTICLE INFO

Article history
Received: 26 July 2020
Accepted: 12 October 2020

Keywords:
Chemical Reaction Parameter, Brownian Motion Parameter, Magnetic Parameter, Darcy Number, Variable Viscosity Parameter and Thermophoresis Parameter

ABSTRACT

In hot and dry climates, evaporative cooling of the air by water spray can be applied in several requirements, such as evaporative condensers which the airflow is precooled by the water spray before it reaches the condenser. The interaction between water droplets and the air is a complicated two-phase flow that is affected by the several parameters. Here, an Eulerian-Lagrangian 3D model was developed to investigate the influence of important parameters on spray cooling performance in a rectangular duct. The evaluated parameters include the number of nozzles, inlet air flow rate, and spray water flow rate. The results represented that growth in the number of nozzles causes a reduction in the spray cooling efficiency. This is due to decrease of droplets retention time within the duct by increasing the number of nozzles at a constant total spray flow rate in the cases. The maximum and minimum spray cooling efficiency belong to the cases with one nozzle at water flow rate of 20 l/h and four nozzle at water flow rate of 5 l/h, respectively. The difference between spray cooling efficiency at 3 and 4 number of nozzles is less than 1.8%. Moreover, increasing the air flow rate from 0.5 l/h to 2 l/h (by 300%) makes a decrease in the spray cooling efficiency up to 58.6%.

Cite this article as: Jagadha S, Gopal D, Vijay KP, Kishan N, Durgaprasad P. Three dimensional mhd nanofluid stagnation point flow with higher order chemical reaction. J Ther Eng 2022;8(2):286–298.

***Corresponding author.**
*E-mail address: jagadhasaravanan@gmail.com, degavath.gopal@gmail.com, vijaykumar.p@vit.ac.in, kishan_n@rediffmail.com, durgaprasad.p@vit.ac.in

* Corresponding Author: durgaprasad.p@vit.ac.in

This paper was recommended for publication in revised form by Regional Editor Erman Aslan

Published by Yıldız Technical University Press, İstanbul, Turkey

INTRODUCTION

This work is focused on mathematical modeling on three dimensional nanofluid on heated vertical surfaces. We investigated MHD stagnation point flow with variable viscosity in the governing fluid flow where nanoparticles are suspended in it. The impact of higher-order chemical reaction of nanofluid flow at a stagnation point in three dimensional is the novelty of the problem. The Brownian motion parameter and thermophoresis parameter are incorporated in the present MHD Nano fluid model. This model helps the industry especially in cooling the devices by analyzing the energy level, is the main investigation of this paper. The physical interpretations of nanofluid flow is extracted in terms of mathematical equations containing partial derivatives along with boundary conditions. The numerical results are obtained by reducing governing equations into coupled nonlinear mathematical ordinary differential equations with transformations using similarity variables. The numerical method Runge-Kutta is employed and computed using MATLAB bvp4c and graphical presentations are obtained for numerical solutions. The effect of dimensionless flow parameters such as order of chemical reaction 'n', magnetic strength M, Darcy number Da, buoyancy parameter N, thermophoretic force parameter Nt, variable viscosity parameter γ_f, Brownian motion parameter Nb in Nano fluid flow, homogeneous chemical reaction process δ are discussed. This investigation revealed that temperature and concentration profile enhance at a large value of the thermophoresis parameter in the nanofluid flow and random Brownian motion parameter develops energy level and decline concentration profile at more values. Comparison of the present results with known numerical results is shown and a good agreement is observed. The heat and mass transfer characteristics were obtained and tabulated. The Nusselt and Sherwood numbers enhance for the dimensionless Nano parameters.

NUMERICAL MODEL

The application of nanofluid plays a vital role in the industry due to its properties such as high thermal conductivity and long-term stability. The important application of nanofluid is electronics cooling, solar collectors, and nuclear applications. Choi presented the concept of nanofluids, to increase thermal conductivity in the flow nanoparticles that are suspended in the fluids Choi and Eastman [1]. A three-dimensional magneto hydro dynamic stagnation point flow of nanofluid influenced by an exponentially stretching surface was studied by Fiaz et al. [2]. A magneto hydro dynamic stagnation point flow of a nanofluid on a plate with an anisotropic slip was discussed by Sadiq et al. [3]. Irfan et al. [4] illustrated the three-dimensional flow of Carreau nanofluid with variable thermal conductivity properties.

Three-dimensional nanofluid effectiveness with Cattaneo-Christov double diffusion by Hayat et al. [5]. Sannad et al. [6] investigated the effects of nanofluid flow in natural convection in three- dimensional direction. Almakki et al. [7] reported on unsteady MHD nanofluid flow with entropy generation in a three-dimensional way. Jusoh et al. [8] studied the effects of nanofluid over a permeable surface in three- dimensional direction flow. Ganga et al. [9] point out deeply MHD with radiation and generating heat impact on nanofluid flow under viscous and ohmic dissipation effects. Ramesh et al. [10] presented the impact of radiation effect; nanoparticles are suspended in the Maxwell fluid with a porous medium in three space coordinates. Madhu et al. [11] observed MHD, viscous dissipation, radiation in three space coordinates with the axisymmetric flow is investigated. Kiyani et al. [12] concentrated on three dimensional mixed convective Williamson nanofluids with chemical reaction.

Hatami et al. [13] viewed three-dimensional nanofluid film on an inclined rotating disk. Rakesh Kumar et al. [14] presented an irreversibility analysis of the fluid flow of carbon nanotubes with radiation and chemical reaction. Sulaiman et al. [15] investigated mass and heat transfer in the nanofluid flow of the Oldroyd-B model in a three-dimensional direction. Muthutamil Selvan et al. [16] analyzed the effects of Lorentz resistive force on three space coordinates micropolar governing flow. Higher or homogeneous chemical processing is influenced by the flow. Zahir Shah et al. [17] characterized nanofluid flow in three space coordinates analyzing the random motion of Brownian and thermophoresis effect in parallel plates.

Kakac et al. [18] presented a thorough review of the increment of heat transfer under the convection medium in nanofluids flow. Fan investigated the role of nano fluid on microreactors. Yu et al. [19] did research on graphene oxide suspending in base fluids to the enhancement of thermal conductivities. Kandasamy et al. [20] discussed MHD mixed convection nanofluid flow under a convective boundary condition. Chandrasekhar Balla et al. [21] pointed out MHD boundary layer flow in an inclined porous square cavity. Nalini et al. [22] reported on nanofluid over stretching sheet under uniform transverse strength of magnetic in the process of chemical reaction. Kuznetsov et al. [23] presented nanofluid surrounded by a plate vertically in the medium of free convection. Jagadha et al. [24] studied Non-Darcy MHD porous medium.

Yirga et al. [25] discussed the effects of MHD, viscous dissipation, reactions in chemical processing, transferring mass, and heat under the influence of porous medium over a stretching sheet. Shafqat Hussain [26] used the finite element method on nanofluid governing flow. He observed that the influence of porous medium effects of viscous dissipation, radiation, and the process of chemical reaction. Gopal et al. [27] observed Brownian and thermophoresis effects on Casson nanofluid over a chemically reacting stretching

sheet with an inclined magnetic field. A non-uniform heat generation or absorption of a stagnation point flow of nanofluid over an exponentially stretching sheet was discussed by Malvandi et al. [28]. Modather et al. [29] demonstrated MHD stagnation point flow in a porous saturated with free convection. He discussed variable viscosity depending on the temperature in three space coordinates. Durga prasad et al. investigated the ability of magneto dynamic strength in the governing fluid flow [30-32]. Jagadha et al. tested MHD nanofluid flow in presence of chemical reaction- [33-35]. Gopal et al. [36] employed the Runge-Kutta method for different geometrical models and resulted in numerically using MATLAB software. Sivaraj [37] analyzed the heat and mass transfer characteristics of cross nanofluid in stagnation point flow over a permeable extending or contracting surface. Gireesha et al. [38] analyzed heat and mass transfer on MHD Casson fluid over a stretching surface. Swain et al. [43] studied by numerical results on MHD nanofluid with slip boundary conditions in presence of higher order chemical reaction. Sadiq [44] discussed the MHD nanofluid stagnation point flow on plate with Anisotropic Slip.

To the best of our knowledge, it is observed that three-dimensional stagnation point nanofluid flow with higher-order chemical reaction is not described in the available literature by researchers. Thus, based on the above research, this study of thermophoresis and Brownian motion effects on the unsteady flow of nanofluid has received a little attention. An effective Runge-Kutta based shooting algorithm is followed to attain the problem's solution. Finally, the results are presented in the form of graphs to discuss the effect of various parameters on the flow field. The extension of the research will take place for the different geometrical models in three dimensions in presence of higher-order chemical reactions in the nanofluid flow. Thus, in the future, the extension work helps the industry to select the mathematical model according to their requirement.

MATHEMATICAL FORMULATION

We investigate three-dimensional steady flow, laminar flow with a magneto hydrodynamic effect. The viscous nanofluid flow is taken along a plane vertically in the medium of a porous state. The stagnation flow is symmetrical about the y-axis and the strength of the magnetic field is normal to y space coordinate. The velocity components (x, y, z) is taken as (u, v, w) respectively. The nanofluid flow is striking effectively on the plate at the point of origin vertically. The initial temperature is assumed as T_w and concentration is taken as C_w constantly in the vertical plate. The nanofluid flow away from the plate at ambient temperature is assumed as T_∞ and C_∞ taken for concentration. The dynamics viscosity is defined as μ, K specifies permeability, density is specified by ρ, the coefficient of expansion of thermal is defined by β_T and the coefficient of concentration expansion is defined by β_c. The diffusion of thermal energy and mass is specified by α and D_m respectively. The governing nanofluid equations are framed considering above mentioned assumptions:

$$\frac{\partial u}{\partial x}+\frac{\partial v}{\partial y}+\frac{\partial w}{\partial z}=0 \tag{1}$$

$$\rho\left(u\frac{\partial u}{\partial x}+v\frac{\partial u}{\partial y}+w\frac{\partial u}{\partial z}\right)=-\frac{\partial p}{\partial x}+\frac{\partial}{\partial x}\left(\mu\frac{\partial u}{\partial x}\right)+\frac{\partial}{\partial y}\left(\mu\frac{\partial u}{\partial y}\right)+\frac{\partial}{\partial z}\left(\mu\frac{\partial u}{\partial z}\right)+\rho g\begin{bmatrix}\beta_T(T-T_\infty)\\+\beta_c(C-C_\infty)\end{bmatrix}-\sigma B^2u-\frac{\mu}{K}u \tag{2}$$

$$\rho\left(u\frac{\partial v}{\partial x}+v\frac{\partial v}{\partial y}+w\frac{\partial v}{\partial z}\right)=-\frac{\partial p}{\partial x}+\frac{\partial}{\partial x}\left(\mu\frac{\partial v}{\partial x}\right)+\frac{\partial}{\partial y}\left(\mu\frac{\partial v}{\partial y}\right)+\frac{\partial}{\partial z}\left(\mu\frac{\partial v}{\partial z}\right)-\frac{\mu}{K}v \tag{3}$$

$$\rho\left(u\frac{\partial w}{\partial x}+v\frac{\partial w}{\partial y}+w\frac{\partial w}{\partial z}\right)=-\frac{\partial p}{\partial x}+\frac{\partial}{\partial x}\left(\mu\frac{\partial w}{\partial x}\right)+\frac{\partial}{\partial y}\left(\mu\frac{\partial w}{\partial y}\right)+\frac{\partial}{\partial z}\left(\mu\frac{\partial w}{\partial z}\right)-\frac{\mu}{K}w \tag{4}$$

$$u\frac{\partial T}{\partial x}+v\frac{\partial T}{\partial y}+w\frac{\partial T}{\partial z}=\alpha\left(\frac{\partial^2T}{\partial x^2}+\frac{\partial^2T}{\partial y^2}+\frac{\partial^2T}{\partial z^2}\right)+\tau\left[D_B\frac{\partial C}{\partial z}\frac{\partial T}{\partial z}+\frac{D_T}{T_\infty}\left(\frac{\partial T}{\partial z}\right)^2\right] \tag{5}$$

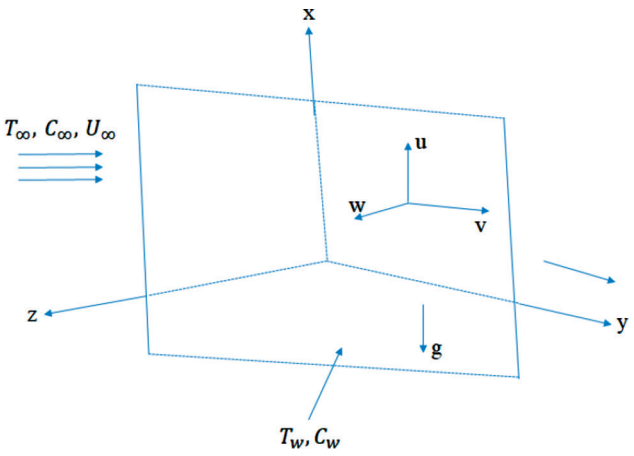

Figure1. Geometry of the problem.

$$u\frac{\partial C}{\partial x}+v\frac{\partial C}{\partial y}+w\frac{\partial W}{\partial z}=D_m\left(\frac{\partial^2 C}{\partial x^2}+\frac{\partial^2 C}{\partial y^2}+\frac{\partial^2 C}{\partial z^2}\right)+\frac{D_T}{T_\infty}\left(\frac{\partial^2 T}{\partial z^2}\right)-K_n\left(C-C_\infty\right)^n \quad (6)$$

The appropriate boundary conditions of the governing flow are defined as:

$$\begin{gathered} u=v=w=0,\ T=T_w\ C=C_w \text{ at } z=0 \\ u=ax,\ v=0,\ w=-ax,\ T=T_\infty,\ C=C_\infty \text{ at } z=\infty \\ p=p_0-\frac{1}{2}\rho a^2\left(x^2+y^2\right) \end{gathered} \quad (7)$$

where *u, v* and are the velocity components of space coordinate system of *x, y* and respectively. Nanofluid pressure is denoted by *p*, p_0 defines stagnation pressure, g is the gravitational force of acceleration, free the streamline separates flow from rest in motion is u_∞. The streamline which separates the fluid from rest in motion is measured to the length of the solid body with inverse proportionality. This is directly proportional to the latent heat of the solid phase and the constant *a*. The absolute viscosity is defined as Carey and Mollendorf [39].

$$\mu=\mu_f\left[1+\frac{1}{\mu_f}\left(\frac{d\mu}{dT}\right)_f\left(T-T_f\right)\right] \quad (8)$$

where μ_f is the film temperature of the nanofluid flow. The governing equations (1)-(6) are transformed into ordinary differential equations with applying appropriate similarity transformation:

$$\eta=\sqrt{\frac{a\rho}{\mu_f}}Z \quad (9)$$

$$u=\frac{g\beta\left(T_\infty-T_w\right)}{a}F(\eta)+axf'(\eta) \text{ and } v=ayf'(\eta) \quad (10)$$

$$w=-2\sqrt{\frac{a\mu_f}{\rho}}f(\eta),T-T_\infty=\left(T_w-T_\infty\right)\theta(\eta),\ C-C_\infty=\left(C_w-C_\infty\right)\varphi(\eta) \quad (11)$$

$$p=p_0-\frac{\rho}{2}\left[a^2\left(x^2+y^2\right)+w^2-2\frac{\mu_f}{\rho}\frac{dw}{dz}\right] \quad (12)$$

Where *F, f,* θ and ϕ are associated to dimensionless functions of nanofluid velocity, nanofluid temperature, and nanofluid concentration respectively.

Substituting Eq. (10) in Eq. (8), we obtain

$$\mu=\mu_f\left[1+\gamma_f(\theta-0.5)\right] \quad (13)$$

$$\gamma_f=\left(\frac{1}{\mu}\frac{d\mu}{dT}\right)_f\left(T_w-T_\infty\right) \quad (14)$$

Employing similarity transformations Eqs.(9)-(12), the continuity eq. (1) is satisfied. The momentum, angular momentum, energy, and concentration equations in three space coordinates are reduced to as follows:

$$\begin{gathered} \left[1+\gamma_f(\theta-0.5)\right]f'''+(2f+\gamma_f\theta)f'' \\ +1-\left(M+\frac{[1+\gamma_f(\theta-0.5)]}{Da}\right)f'= \\ \left[1+\gamma_f(\theta-0.5)\right]F''+(2f+\gamma_f\theta)F'+fF \\ -N\varphi-\left(M+\frac{[1+\gamma_f(\theta-0.5)]}{Da}\right)F \end{gathered} \quad (15)$$

$$\frac{1}{\mathrm{Pr}}\theta''+2f\theta'+Nt\theta'^2+Nb\theta'\varphi'=0 \quad (16)$$

$$\frac{1}{Sc}\varphi''+2f\varphi'+\frac{1}{Sc}\frac{Nt}{Nb}\theta''-\Gamma\varphi''=0 \quad (17)$$

Where Darcy number is denoted by $Da = K\rho a/\mu_f$, buoyancy parameter is denoted by $N = \beta_c (C_w - C_\infty)/\beta_T (T_w - T_\infty)$, specifies Prandtl number is $Pr = C_p\mu_f/k$, specifies Schmidt number $Sc = \mu_f/D_m$, magnetic parameter is $M = \sigma B^2/a\rho$, Thermophoresis parameter is denoted by $Nt=\frac{\tau D_T\left(T_w-T_\infty\right)}{\nu T_\infty}$, Brownian motion parameter is defined by $Nb=\frac{\tau D_T\left(C_w-C_\infty\right)}{\nu}$, chemical reaction parameter $\delta=\frac{K_n\left(C_w-C_\infty\right)^{n-1}}{a}$, Kinematic viscosity $\nu=\frac{\mu_f}{\rho}$.

Primes represent differentiation of η. The transformed nanofluid boundary layer conditions are:

$$f(0)=f'(0)=F(0)=0,\theta(0)=1,\varphi(0)=1 \quad (18)$$

$$f'(\infty)=1,F(\infty)=\theta(\infty)=\varphi(\infty)=0 \quad (19)$$

The shear stress, heat and mass flux are:

$$\tau_{wx}=\left(\mu\frac{\partial u}{\partial z}\right)_{z=0}=\mu_f\left[F'(0)\frac{g\beta(T_\infty-T_w)}{a}+axf''(0)\right]\left(1+0.5\gamma_f\right)\sqrt{a\rho/\mu_f} \quad (20)$$

$$\tau_{wx} = \left(\mu \frac{\partial v}{\partial z}\right)_{z=0} = \mu_f \left(1 + 0.5\gamma_f\right) \sqrt{a\rho/\mu_f}\, ayf''(0) \quad (21)$$

$$q_w = -k\left(\frac{\partial T}{\partial z}\right)_{z=0} = -k\sqrt{a\rho/\mu_f}\left(T_w - T_\infty\right)\theta'(0) \quad (22)$$

$$m_w = -D_m\left(\frac{\partial C}{\partial z}\right)_{z=0} = -D_m\sqrt{a\rho/\mu_f}\left(C_w - C_\infty\right)\varphi'(0) \quad (23)$$

Then the Nusselt number and Sherwood number are:

$$Nu = -\sqrt{a\rho/\mu_f}\,\theta'(0), Sh = -\sqrt{a\rho/\mu_f}\,\varphi'(0) \quad (24)$$

$$\text{Here } Nu = \frac{q_w x}{\left(T_w - T_\infty\right)k} \text{ and } Sh = \frac{m_w x}{\left(C_w - C_\infty\right)D_m} \quad (25)$$

Here wall heat and mass flux defined as q_w and m_w.

NUMERICAL METHOD

The numerical method Runge-Kutta fourth-order is used to solve non-linear ordinary differential equations (14-16) with appropriate boundary conditions (17). A set of non-linear ordinary differential equations are obtained in the form of third order, F second order, θ and ϕ. The reduction of above non-linear differential equations leads to simultaneous equations. Moreover, the values of f', F, θ, ϕ are presented when $\eta \to \infty$. With the help of these end conditions, the unknown initial conditions at $\eta \to 0$ using shooting technique. In the shooting method, the boundary value problems are reduced into to an initial value problem by assuming initial values. The calculation of boundary value should match with the real boundary value as possible. The most important step is to select the appropriate finite value of boundary condition far field. We presented infinity condition at a large but finite value of η, there is no variation in velocity, angular velocity, temperature, and concentration. We computed a maximum value of $\eta = 5$ which is sufficient to get the target of far-field boundary conditions asymptotically for all values of nondimensional parameters considered.

Introducing new variables for the conversion of higher order to linear differential equation.

$$\begin{aligned} &f_1 = f,\ f_2 = f^{'},\ f_3 = f^{''},\ f_4 = F, f_5 = F', \\ &f_6 = \theta,\ f_7 = \theta^{'},\ f_8 = \phi, f_9 = \phi^{'} \end{aligned} \quad (26)$$

The equations (14)-(17) are transformed to following first order ODE.

$$\begin{aligned} f_3 = &-(1/(1 + Gff_6 - 0.5Gf))(2f_1f_3 + Gff_3f_7 - f_2f_2 - Mf_2 \\ &+ (1/Da)f_2 + (Gf/Da)f_6f_2 - 0.5(Gf/Da)f_2) \end{aligned} \quad (27)$$

$$\begin{aligned} f_5 = &-(1/(1 + Gff_6 - 0.5Gf))(2f_1f_5 + Gf_5f_7 - f_1f_7 - Nf_7 - f_6 \\ &- Mf_4 + (1/Da)f_4 + (Gf/Da)f_4f_6 - 0.5(Gf/Da)f_4) \end{aligned} \quad (28)$$

$$f_7 = -2\,\mathrm{Pr}\, f_1f_7 + Ntf_7f_7 + Nbf_7f_9 \quad (29)$$

$$f_9 = -2Scf_1f_9 + \frac{1}{Sc}\frac{Nt}{Nb}f_7 - kf_8 \quad (30)$$

The approximate solutions are numerically resulted using MATLAB bvp4c programming to present the physical significance of non-dimensional parameters.

RESULTS AND DISCUSSION

In this research study, higher-order chemical reaction of order impact on three space coordinate nanofluid flow investigated numerically. To obtain the result, we employed a numerical scheme Runge-Kutta method using MATLAB software bvp4c. Calculations are put out for the fixed values (γ_f = 2, N = 2, Pr = 0.7, M = 1, Sc = 2, δ = 2, Nt = 2, Nb = 2, n = 1, Da = 1) of Brownian motion parameter Nb, magnetic parameter M, Darcy number Da, buoyancy parameter N, thermophoresis parameter Nt, chemical reaction parameter δ, n represents process of chemical reaction with order and variable viscosity range γ_f, Prandtl number Pr, Schmidt number Sc analyzed and physical interpretation of dimensionless numbers graphically.

Firstly, we investigated the effect of magnetic parameter M versus $f'(\eta)$, $F'(\eta)$, $\theta(\eta)$ and $\varphi(\eta)$. The effects of the magnetic parameter are displayed graphically in Figures 2 (a-d). It is visualized that the curves of both $f'(\eta)$, $F'(\eta)$ are decay with enhance of magnetic parameter M in Figures 2 (a-b). Further Figures 2 (c) and 2 (d) present a reverse effect on the $\theta(\eta)$ and $\varphi(\eta)$. We noticed that the strength of the magnetic parameter M induces a force named Lorentz force. This resistive force opposes the governing flow which tends to slow down the nanofluid flow. Thus, the effect of M decreases the nanofluid velocity, nanofluid angular velocity, and also causes enhance in temperature and concentration distributions. This impact is summarized magnetic parameter ranging from 0 to 2. If variable viscosity influence is more or the magnetic parameter range increase, the curves are not in a proper manner.

The influence of thermophoretic force, heat transfer on nanofluid flow, and mass transfer on nanofluid is presented in Figures 3 (a-b). It is noteworthy that temperature increases with an increase in Nt and its related boundary layer thickness. Large values of the thermophoresis parameter provide more heat to the nanofluid leads to a decline in a concentration gradient. If the viscosity level increases along with more heated, then the governing flow is not in order in both temperature and concentration profiles.

Figures 4(a) and 4(b) represent the physical significance of Brownian motion on nanofluid temperature and nanofluid concentration profiles. We examine from the figure that the θ associated nanofluid thermal level is increased when Nb enhances. The concentration φ and the associated nanofluid species level also enhances when the Brownian motion parameter increases due to the influence of chemical reaction. The influence of the order of chemical reaction with Brownian motion, the collision between nanoparticles and random motion exhibit concentration gradient decline.

The impact of Darcy number Da on velocity and angular velocity profiles is plotted in Figures 5(a) and 5(b). It is evident that the larger values of Da cause enhance in both f' and F' distribution. The viscous in the nanofluid motion causes both profiles to enhance when increasing Darcy parameter value in the governing flow.

The effects of variable viscosity parameter γ_f on f' and F' can be demonstrated in Figures 6(a) and 6(b). It is anticipated by these figures that velocity distribution diminishes near the nanofluid boundary layer and enhances far away from the nanofluid boundary layer. The opposite behavior

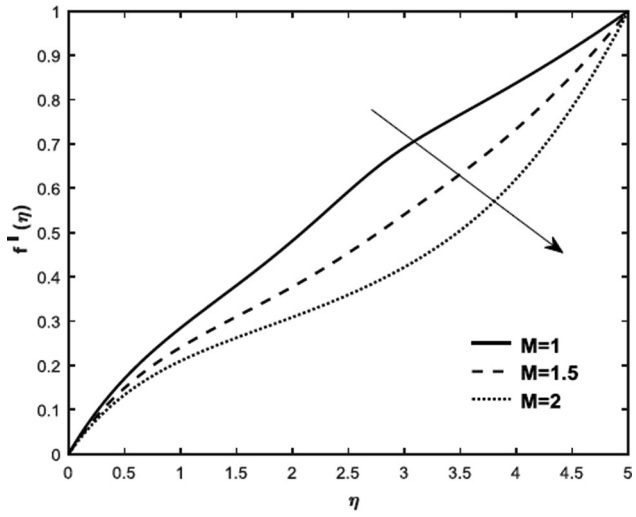

Figure 2(a). Effects of magnetic parameter on velocity profile.

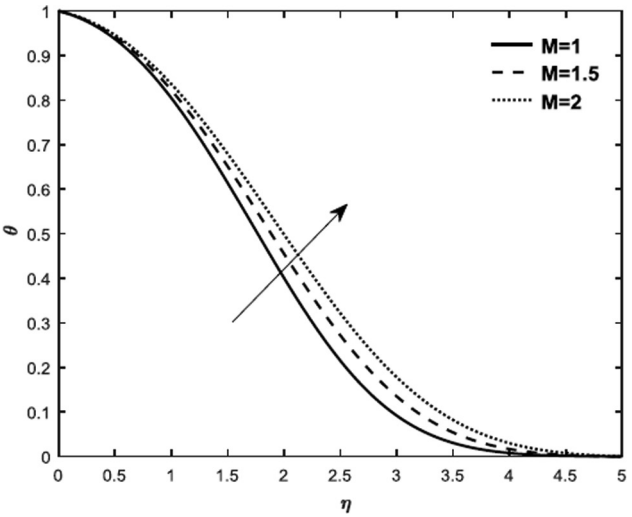

Figure 2(b). Effects of magnetic parameter on temperature profile.

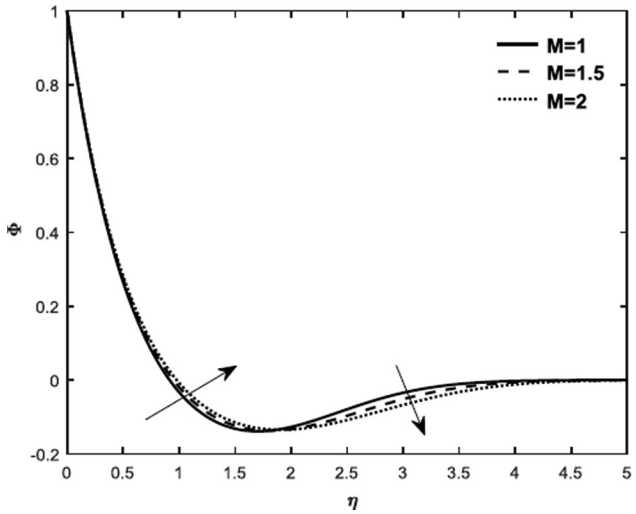

Figure 2(c). Effects of magnetic parameter on concentration profile.

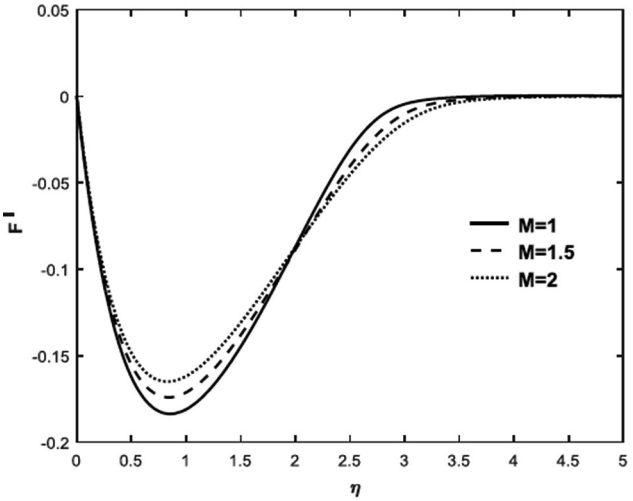

Figure 2(d). Effects of Magnetic parameter on angular velocity profile.

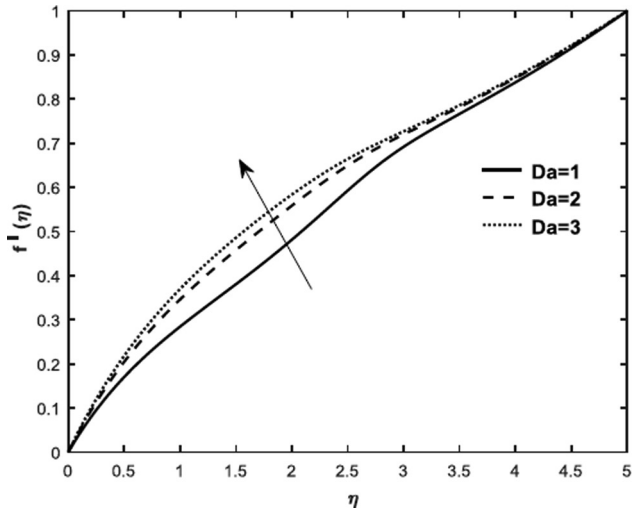

Figure 3(a). Effects of Darcy number on velocity profile.

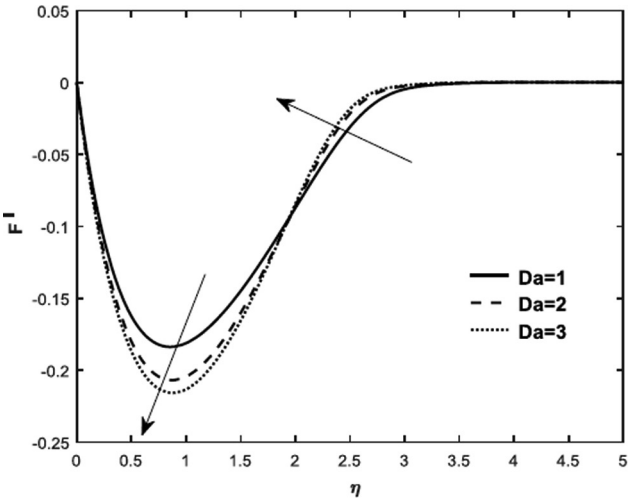

Figure 3(b). Effects of Darcy number on angular velocity profile.

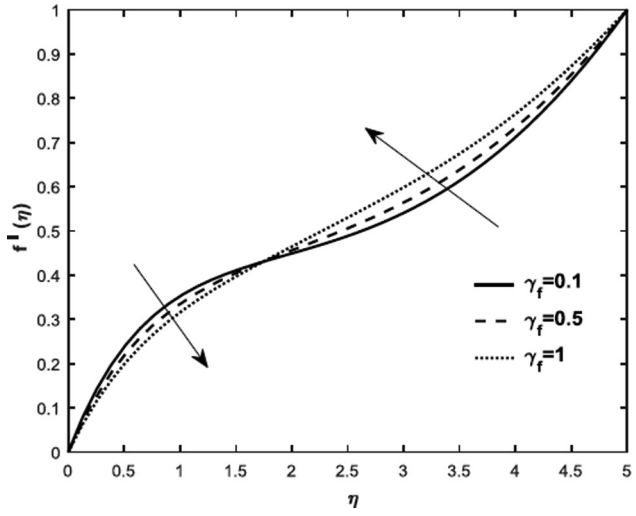

Figure 4(a). Effects of variable viscosity on velocity profile.

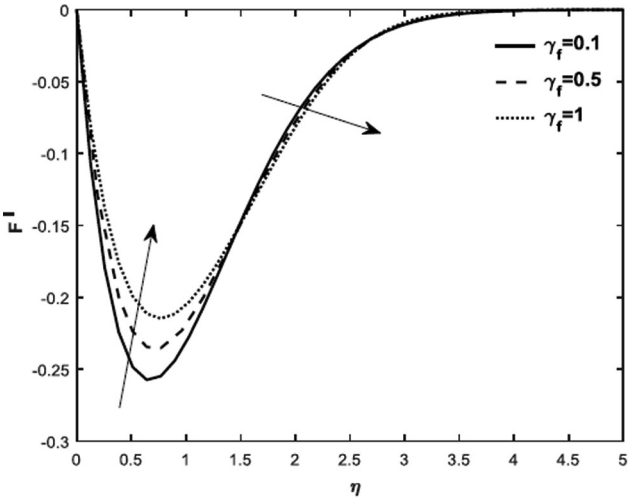

Figure 4(b). Effects of variable viscosity on angular viscosity profile.

in the governing angular velocity gradient due to the influence of pressure gradient and viscosity associated dimensionless number Darcy effect in the governing nanofluid flow region.

Figure 7 demonstrates the behaviour of the nanofluid concentration profile on the dimensionless number homogeneous process of reaction chemically. The species concentration of nanofluid is a decreasing function of δ. The random nanofluid motion of Brownian with the processing of homogeneous chemical reaction provides a diminishing concentration gradient.

The effect of the Prandtl number is shown in Figurees 8 (a) and 8 (b). The dimensionless number Prandtl is related to viscous diffusion rate and thermal diffusion, the larger value of Prandtl enhances the temperature gradient and reduces the concentration gradient which is at a distance away from the nanofluid boundary layer.

The impact of *Sc* on mass transfer profile is displayed in Figure 9. The physical significance of *Sc* is the ratio of diffusion of mass and kinematic viscosity. The domination of kinematic viscosity in the governing nanofluid flow plays a significant effect on the increasing function of the Schmidt

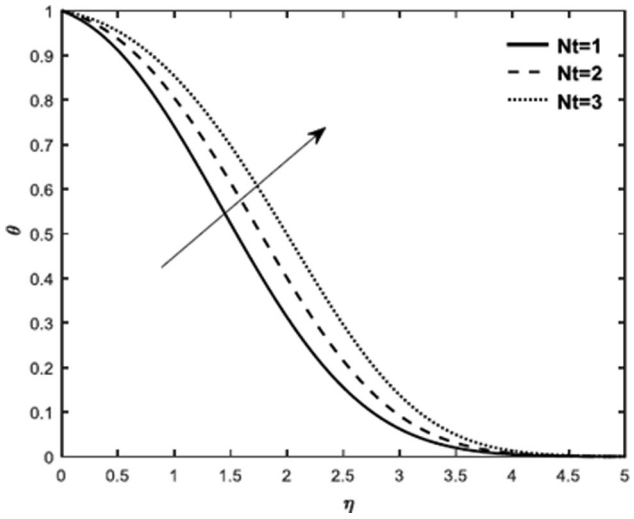

Figure 5(a). Effects of Thermophoresis parameter on temperature profile.

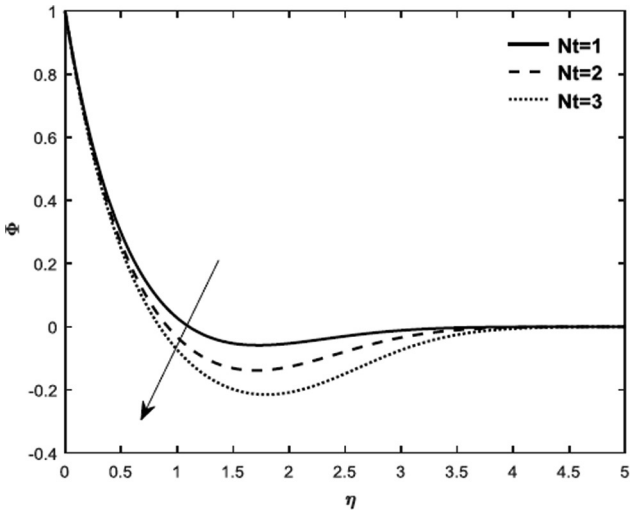

Figure 5(b). Effects of thermophoresis parameter on concentration profile.

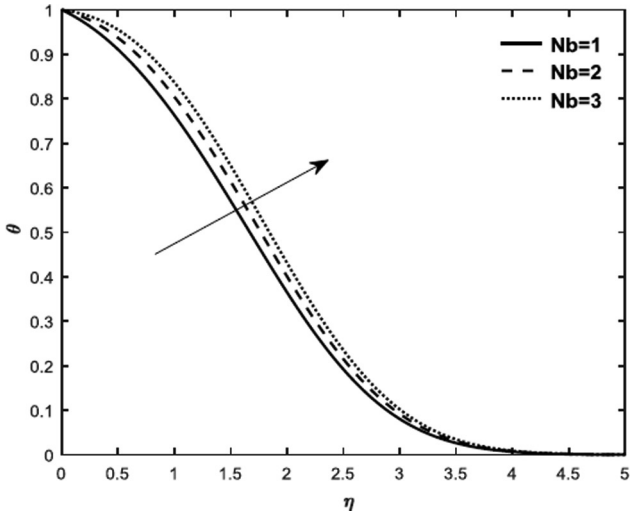

Figure 6(a). Effects of Brownian motion in temperature profile.

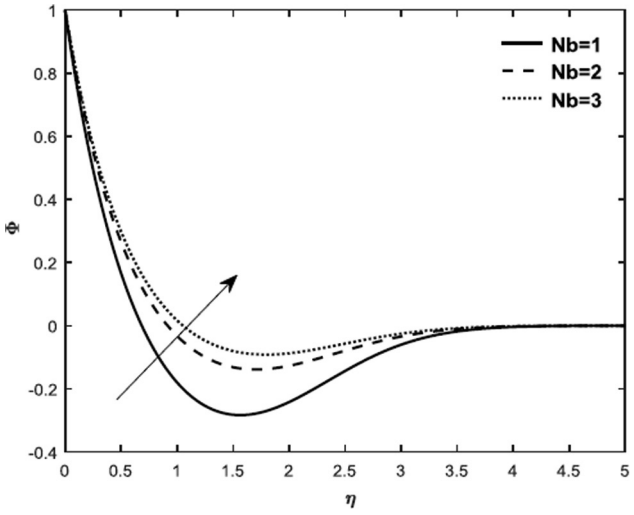

Figure 6(b). Effects of Brownian motion in concentration profile.

number. Thus, we observed a decline in the concentration gradient.

The order of homogeneous chemical reaction parameter governs the nanofluid flow is shown in Figure 10. The mass transfer increases when chemical processing in increasing level with the order. The physical interpretation of the random motion of fluid and chemical processing.

Table 1 illustrates that the comparison of the present results with those reported by Zaimi et al. [40], Yasin et al. [41], Gopal et al. [42]. Here seen an excellent agreement between these results.

The numerical values are presented for various values of dimensionless numbers as a function of Prandtl number, which are closed to the published journals. The error is very minor. Also, Table 2 deals with differences of Nusselt number and Sherwood number with various values of γ_f, *M*, *Da*, *N, Nt, Nb,* δ and *Sc*. It is clear that the Nusselt number increasing with encouraged values of γ_f, *M*, *Da*, *Nb,* δ,

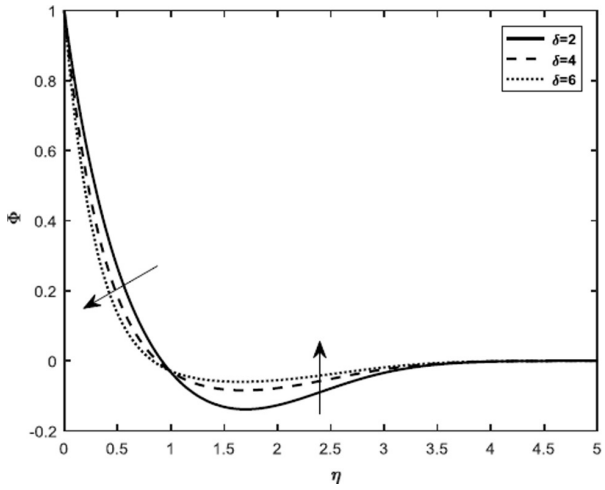

Figure7. Effects of chemical reaction parameter in concentration profile.

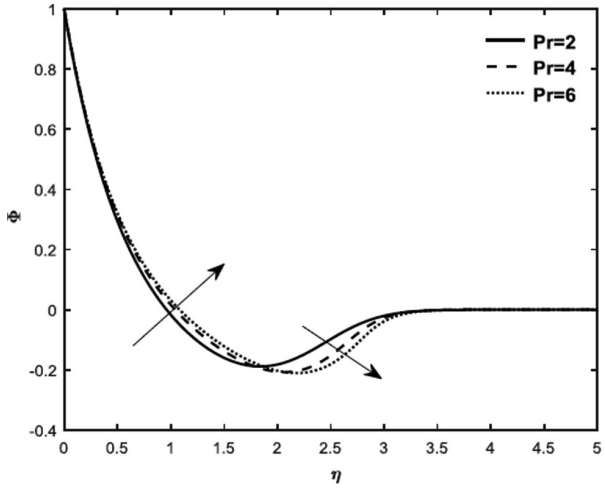

Figure 8(b). Effects of Prandtl number on concentration profile.

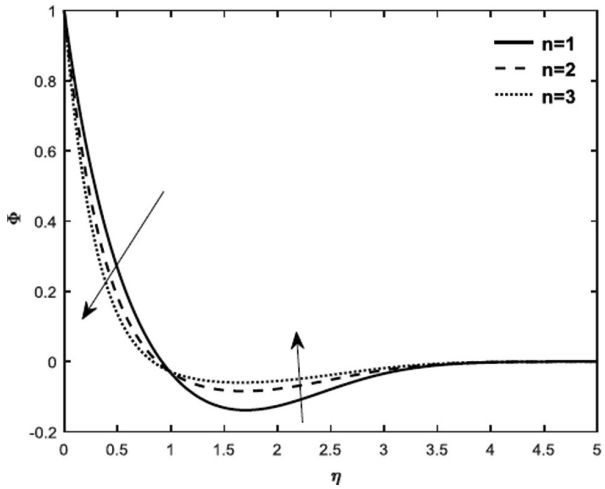

Figure 10. Effects of order of chemical reaction parameter on concentration profile.

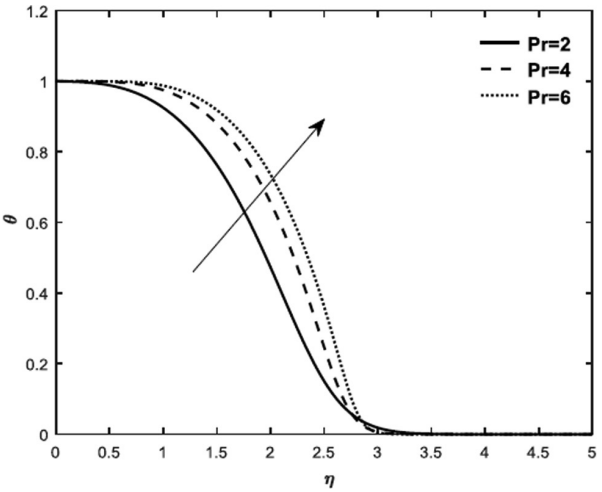

Figure 8(a). Effects of Prandtl number on temperature profile.

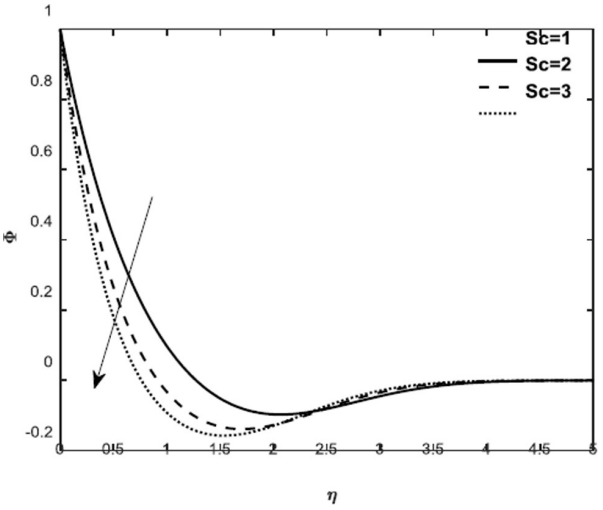

Figure 9. Effects of Schmidt number on concentration profile.

Table 1. Comparison with previous published data for the values of $-\theta'(0)$ when $\gamma_f = 0.1$, $M = 2$, $Da = 0.3$, $N = 0.1$, $Nt = 0.3$, $Nb = 0.8$, $Sc = 0.66$ and $\delta \to \infty$

Pr	0.72	1	3	5
Zaimi et al. [40]	0.463145	0.581977	1.165246	-
Yasin et al. [41]	0.4631	0.5820	1.1652	1.5681
Gopal et al. [42]	0.463254	0.581983	1.165253	1.568063
Present	0.463263	0.581842	1.165192	1.567915

Sc and rest of parameters are buoyancy parameter (*N*) and thermophoresis parameters (*Nt*) opposite behaviour exist. On the other hand, magnetic, thermophoresis, Brownian motion parameters and Darcy number are enhancing Sherwood number and rest of parameters are opposite behavior exist.

Table 2. Variants in Nusselt number and Sherwood number for various values of $\gamma_f = 0.5$, $M = 2$, $Da = 0.3$, $N = 0.1$, $Nt = 0.3$, $Nb = 0.8$, $\delta = 0.5$, $Sc = 0.6$.

γ_f	M	Da	N	Nt	Nb	δ	Sc	$-\sqrt{\frac{a\rho}{\mu_f}}\theta'(0)$	$-\sqrt{\frac{a\rho}{\mu_f}}\varphi'(0)$
-0.5	2.0	0.3	0.1	0.3	0.8	0.6	0.4	0.019953	8.915563
0.0								0.748988	5.028091
0.5								0.996884	4.053773
	0.5							0.766466	2.610498
	1.5							0.931372	3.653716
	2.5							0.987861	5.809726
		1.0						0.179721	5.990796
		2.0						0.360588	6.601553
		5.0						0.465598	6.826009
			0.1					1.085478	4.109033
			0.4					0.557416	4.109033
			0.9					0.095219	4.109033
				0.6				0.864902	16.250231
				1.2				0.838678	21.485467
				1.8				0.803155	28.270380
					0.8			0.857340	17.844717
					1.6			1.003571	29.783310
					2.5			1.173758	55.715972
						0.4		0.869876	14.149107
						1.4		0.872763	14.065691
						2.4		0.890472	14.030153
							1.0	0.843848	14.467089
							2.0	0.846561	14.428440
							4.0	0.856025	14.306650

CONCLUSION

In the present investigation, we studied three-dimensional nanofluid on heated vertical surfaces, MHD stagnation point flow with variable viscosity in the governing fluid flow where nanoparticles are suspended in it. The impact of the higher-order chemical reaction is observed. The numerical results are obtained by reducing governing equations into coupled nonlinear mathematical ordinary differential equations with similarity transformations. The numerical results have been reported for the geometrical model under the influence of variable viscosity parameter, Brownian motion parameter, Darcy number, thermophoresis parameter, Schmidt number, dimensionless Prandtl number, and dimensionless chemical reaction parameter. The physical significance of these parameters is given numerically by using the R-K method and presented graphically with the aid of MATLAB software bvp4c.

- The significant effect more in velocity profile and angular velocity profile for the increment of Darcy number and whereas declined by Magnetic parameter.
- Brownian motion parameter, Magnetic parameter, and thermophoresis parameter and enhance temperature in fluid flow due to that temperature profile increases
- The concentration profile enhances with an increment of Brownian motion parameter, range of chemical processing with order, and magnetic parameter. The declining trend is observed in the boundary layer species profile for the insight of the parameters such as thermophoresis parameter, Schmidt number, Prandtl number, and chemical reaction parameter.
- The Nusselt number enhances with dimensionless parameters γ_f, M, Da, Nb, δ, Sc except (N) and (Nt).

- The growth of Sherwood number is noticed in magnetic, thermophoresis, Brownian motion parameters and Darcy number.
- Prandtl number escalates the temperature distribution, therefore increases the thermal boundary layer thickness.
- The numerical data is listed for different values of dimensionless numbers as a function of Prandtl number, which ensure good agreement to the published journals.

NOMENCLATURE

u, v, w : Velocity components in directions (m/s)
x, y, z : Space coordinates (m)
B_0 : Uniform magnetic field (Tesla)
T : Temperature of fluid (K)
T_w : Temperature at the surface (K)
T_∞ : Ambient temperature (K)
C : Concentration of fluid (kg/m^3)
C_w : Concentration at the surface (kg/m^3)
C_∞ : Ambient concentration (kg/m^3)
D_B : Brownian diffusion coefficient
D_T : Thermophoresis diffusion coefficient
U_w : Stretching sheet velocity (m/s)
g : Gravity (m/s^2)
ρ : Fluid density (kg/m^3)
p : Nanofluid pressure
α^* : Thermal diffusivity Coefficient (m^2/s)
α : Thermal energy
f : Dimensionless stream function
Nb : Brownian motion parameter
Nt : Thermophoresis parameter
σ : Electrical conductivity of the fluid (m/s)
Sr : Soret number
δ : Chemical reaction coefficient
C_p : Specific heat at constant pressure (J/kg K)
Ec : Eckert number
Pr : Prandtl number
Nu : Local Nusselt number
Sh : Sherwood number
Re : Local Reynolds number
q_w : Surface heat flux
μ : Dynamic viscosity (N/m^2)
μ_0 : Zero shear viscosity (s^{-1})
μ_∞ : Infinite shear viscosity (s^{-1})
ν : Kinematic viscosity (m^2/s)
μ : Dynamic viscosity (N s/m^2)
ψ : Stream function
F, f : Dimensionless nanofluid velocity
θ : Dimensionless nanofluid temperature
ϕ : Dimensionless nanofluid concentration function
η : Dimensionless similarity variable

Subscripts
∞ : Ambient condition
w : Condition on surface

Superscript
$'$: Differentiation with respect to η

AUTHORSHIP CONTRIBUTIONS

Authors equally contributed to this work.

DATA AVAILABILITY STATEMENT

The authors confirm that the data that supports the findings of this study are available within the article. Raw data that support the finding of this study are available from the corresponding author, upon reasonable request.

CONFLICT OF INTEREST

The author declared no potential conflicts of interest with respect to the research, authorship, and/or publication of this article.

ETHICS

There are no ethical issues with the publication of this manuscript.

REFERENCES

[1] Choi SUS, Eastman JA. Enhancing thermal conductivity of fluids with nanoparticles. ASME Int. Mech Eng Cong Expo 1995;66:99–105.
[2] Rehman FU, Nadeem S, Rehman HU, Ul Haq R. Thermophysical analysis for three-dimensional MHD stagnation-point flow of nano-material influenced by an exponential stretching surface. Results Phys 2018;8:316–323. [CrossRef]
[3] Sadiq MA. MHD stagnation point flow of nanofluid on a plate with Anisotropic slip. Symmetry 2019;11:132. [CrossRef]
[4] Irfan M, Khan M, Khan WA. Numerical analysis of unsteady 3D flow of Carreau nanofluid with variable thermal conductivity and heat source/sink. Results Phys 2017;7:3315–3324. [CrossRef]
[5] Hayat T, Ayub T, Taseer M, Ahmed Alsaedi. Three-dimensional flow with Cattaneo-Christov double diffusion and homogeneous-heterogeneous reactions. Results Phys 2017;7:2812–2820. [CrossRef]

[6] Sannad M, Abourida B, Belarche L, Doghmi H, Mouzaouit. Natural convection in a three-dimensional cavity filled with nanofluid and partially heated: Effect of the hating section dimension. IOP Conf Ser: Mater Sci Eng 2015;186:19–21. [CrossRef]
[7] Almakki M, Dey S, Mondal S, Sibanda P. On unsteady three-dimensional axisymmetric MHD nanofluid flow with entropy generation and thermo-diffusion effects on a non-linear stretching sheet. Entropy 2017;19:168. [CrossRef]
[8] Jusoh R, Nazar R, Pop I. Three-dimensional flow of a nanofluid over a permeable stretching/shrinking surface with velocity slip: A revised model. Phys Fluids 2018;30:033604. [CrossRef]
[9] Ganga B, Ansari SMY, Ganesh NV, Hakeem AKA. MHD radiative boundary layer flow of nanofluid past a vertical plate with internal heat generation/absorption, viscous and ohmic dissipation effects. J Niger Math Soc 2015;34:181–194. [CrossRef]
[10] Ramesh GK, Prasannakumara BC, Gireesha BJ, Shehzad SA, Abbasi FM. Three-dimensional flow of Maxwell fluid with suspended nanoparticles past a bidirectional porous stretching surface with thermal radiation. Thermal Science and Engineering Progress 2017;1:6–14. [CrossRef]
[11] Madhu M, Balaswamy B, Kishan N. Three-dimensional MHD boundary layer flow due to an axisymmetric shrinking sheet with radiation, viscous dissipation and heat source/sink. Int J Appl Mech Eng 2016;26:393–406. [CrossRef]
[12] Hayat T, Kiyani MZ, Alsaedi A, Ijaz Khan M, Ahmad I. Mixed convective three-dimensional flow of Williamson nanofluid subject to chemical reaction. Int J Heat Mass Transf 2018;127:422–429. [CrossRef]
[13] Hatami M, Jing D, Majeed A, Yousif. Three-dimensional analysis of condensation nanofluid film on an inclined rotating disk by efficient analytical methods. Arab J Basic Appl Sci 2018;25:28–37. [CrossRef]
[14] Kumar R, Kumar R, Sheikholeslami M, Chamkha AJ. Irreversibility analysis of the three-dimensional flow of carbon nanotubes due to nonlinear thermal radiation and quartic chemical reactions. J Mol Liq 2019;274:379–392. [CrossRef]
[15] Sulaiman M, Aamir Ali, Islam S. Heat and mass transfer in three-dimensional flow Oldroyd-B nanofluid with Gyrotactic micro-organisms. Math Probl Eng 2018;9:1–15. [CrossRef]
[16] Muthutamilselvan M, Ramya E, Deog-Hee D. Inclined Lorentz force effects on 3D micropolar fluid flow due to a stretchable rotating disk with higher order chemical reaction. J Mech Eng Sci 2018;233:323–335. [CrossRef]
[17] Shah Z, Gul T, Islam S, Khan MA, Bonyah E, Hussain F, Mukhtar S, Ullah M. Three-dimensional third grade nanofluid flow in a rotating system between parallel plates with Brownian motion and thermophoresis. Results Phys 2018;10:36-45. [CrossRef]
[18] Kakac S, Pramuanjaroenkij A. Review of convective heat transfer enhancement with nanofluids. Int J Heat Mass Transf 2009;52:3187–3196. [CrossRef]
[19] Yu W, Xie H, Bao D. Enhanced thermal conductivities of nanofluids containing graphene oxide nanosheets. Nanotechnology 2010;21:055705. [CrossRef]
[20] Kandasamy R, Jeyabalan C, Sivagnana Prabhu KK. Nanoparticle volume fraction with heat and mass transfer on MHD mixed convection flow in a nanofluid in the presence of thermo-diffusion under convective boundary condition. Appl Nanosci 2016;6:287–300. [CrossRef]
[21] Balla CS, Kishan N, Gorla RSR, Gireesha BJ. MHD boundary layer flow and heat transfer in an inclined porous square cavity filed with nanofluids, Ain Shams Eng J 2017;8:237–254. [CrossRef]
[22] Nalini SP, Vishwmbhar SP, Salunke JN. Nanofluid under uniform transverse magnetic field with a chemical reaction past a stretching sheet. Int J Math Trends Technol 2017;51:336–342. [CrossRef]
[23] Kuznetsov AV, Nield DA. Natural convective boundary layer flow of a nanofluid past a vertical plate: A revised model. Int J Therm Sci 2014;77:126–129. [CrossRef]
[24] Jagadha S, Hymavathi D, Kishan N. MHD mixed convection non-Darcy porous medium saturated with a nanofluid under the influence radiation. J Nanofluids 2016;5:302–309. [CrossRef]
[25] Yirga Y, Tesfay D. Heat and Mass Transfer in MHD flow of nanofluids through a porous media due to a permeable stretching sheet with viscous dissipation and chemical reaction effects. Int J Mech Mechatron Eng 2015;9:709–716.
[26] Hussain S. Finite element solution for MHD flow of nanofluids with heat and mass transfer through a porous media with thermal radiation, viscous dissipation and chemical reaction effects. Advances in Applied Mathematics and Mechanics 2017; 9: 904–923. [CrossRef]
[27] Gopal D, Kishan N. Brownian motion and Thermophoresis effects on Casson Nanofluid over a chemically reacting stretching sheet with inclined magnetic field. Adv Appl Math Mech 2019;4:106–116.
[28] Malvandi A, Hedayati F, Domairry G. Stagnation point flow of a nanofluid toward an exponentially stretching sheet with nonuniform heat generation/absorption. J Thermodyn 2013;764827. [CrossRef]
[29] Modather M, Abdou M, El-Kabier M. Magneto-Hydrodynamic Effect with Temperature Dependent Viscosity on Natural Convection at an axisymmetric

stagnation point saturated in porous media. Adv Theor Appl Mech 2014;7:1–20. [CrossRef]

[30] Durga Prasad P, Sivaraj R, Madhusudhana Rao B, Raju CSK, Venkateswara Raju K, Varma SVK. Unsteady Casson MHD Flow Due to Shrinking Surface with Suction and Dissipation. In: Rushi Kumar B, Sivaraj R, Prakash J. (Eds,). Advances in Fluid Dynamics. Lecture Notes in Mechanical Engineering. Springer, Singapore, 2021:559–572. [CrossRef]

[31] Venkateswara Raju R S K, Durga Prasad P, Raju M C. MHD Casson Fluid Flow past a stretching sheet with convective boundary and heat source, Lecture notes in Mechanical Engineering 2020; 549–558. [CrossRef]

[32] Venkateswarlu S, Varma SVK, Durga Prasad P. MHD flow of MoS_2 and MgO water-based nanofluid through porous medium over a stretching surface with Cattaneo-Christov heat flux model and convective, Int J Ambient Energy 2020; 559–572. [CrossRef]

[33] Jagadha S, Gopal D, Kishan N. Nanofluid flow of higher order radiation chemical reaction with effects of melting and viscous dissipation. J Phys Conf Ser 2020;1451:012003. [CrossRef]

[34] Jagadha S, Gopal D, Kishan N. Soret and Dufour effects of electrical MHD Nanofluid with higher order chemical reaction. Test Eng Manag 2020;82:2250–2259.

[35] Jagadha S, Kalyani K, Kishan N. Viscous and Ohmic dissipation on non-Darcy MHD nanofluid mixed convection flow in porous medium with suction/injection effects. J Phys Conf Ser 2019;1172:012014. [CrossRef]

[36] Gopal D, Naik SHS, Kishan N, Raju CSK. The impact of thermal stratification and heat generation absorption on MHD carreau nanofluid flow over a permeable cylinder. SN Appl Sci 2020;2:639. [CrossRef]

[37] Bash HT, Sivaraj R. Heat and mass transfer in stagnation point flow of cross nanofluid over a permeable extending/contracting surface: A stability analysis. J Therm Eng 2022;8:38–51. [CrossRef]

[38] Gireesha B J, Mahanthesh B, Rashidi, MHD boundary layer heat and mass transfer of a chemically reacting Casson fluid over a permeable stretching surface with non-uniform heat source, International Journal of Industrial Mathematics 2015;7:247–260.

[39] Carey PV, Mollendorf CJ. Natural convection in liquids with temperature dependent viscosity. Proceedings of the Sixth International Heat Transfer Conference 1978;2:211–217. [CrossRef]

[40] Zaimi K, Ishak A, Pop I. Flow past a permeable stretching/shrinking sheet in a nanofluid using two-phase model. PLoS One 2014;19:111–743. [CrossRef]

[41] Hafizi Mat YM, Anuar I, Ioan P. MHD heat and mass transfer flow over a permeable stretching/shrinking sheet with radiation effect. J Magn Magn Mater 2016;407:235–240. [CrossRef]

[42] Gopal D, Kishan N, Raju CSK. Viscous and Joule's dissipation on Casson fluid over a chemically reacting stretching sheet with inclined magnetic field and multiple slips. Informatics in Medicine Unlocked 2017;9:154–160. [CrossRef]

[43] Swain K, Parida SK, Dash GC. Higher order chemical reaction on MHD nanofluid flow with slip boundary conditions: A numerical approach. Math Model Eng Probl 2019;6:293–299. [CrossRef]

[44] Sadiq M.A. MHD Stagnation point flow of nanofluid on a plate with anisotropic slip. Symmetry 2019;11:132. [CrossRef]